CLM - R 162

CLM - R 162

UKAEA RESEARCH GROUP

Report

ENHANCED REIONISATION LOSS FOR NEUTRAL BEAMS IN MAGNETIC FIELDS

R S HEMSWORTH

CULHAM LABORATORY
Abingdon Oxfordshire

1977

Available from H. M. Stationery Office

C/18

50p.

UDC: 539.188:537.56

CLM - R162

ENHANCED REIONISATION LOSS FOR NEUTRAL BEAMS IN MAGNETIC FIELDS

by

R. S. Hemsworth
Culham Laboratory, Abingdon OX14 3DB, England
(Euratom/UKAEA Fusion Association)

ABSTRACT

Enhanced loss of neutral beam particles is caused by an increase in the background gas target density by desorptions from the tube wall when reionised particles are deflected in the presence of a magnetic field. Inconsistencies in the original treatment of the problem are removed by the present analysis which predicts a factor two higher maximum possible transmitted equivalent beam current.

April 1976

SBN: 85311 048 4

1. INTRODUCTION

Intense neutral beams are used for heating plasma in magnetic confinement devices. Riviere and Sheffield[1] have shown that attenuation of the beam may occur during transit through the input tube which is immersed in the magnetic field of the experimental device. Beam atoms are ionised by collisions with gas molecules and these ions are deflected into the walls by the magnetic field. Gas desorbed by this bombardment adds to the ionisation target, more beam atoms are ionised and so on. Unfortunately there are inconsistencies in the treatment of Riviere and Sheffield. Briefly, if the terms are as defined, their equation (1) refers to the central density in the pipe, not the mean density as stated, and the initial gas density is inadequately defined in equation (2). However, the basic conclusion of their 'time dependent solution' that steady state situations are set up in a few milliseconds is obviously correct. The following analysis of the steady state situation removes the inconsistencies of the previous treatment.

2. ANALYSIS

The situation considered is as in Fig. 1. The following are assumed:

1. The beam approaching the input pipe is completely neutral, i.e. any charged fraction has been removed prior to the pump.
2. All the gas desorbed by the ion bombardment is evolved half way along the input tube.
3. The ion source gas efficiency is independent of the extracted current.
4. Pressures in the system are such that molecular flow conditions prevail.
5. The gas desorbed from the input tube is the same as that from the ion source.
6. The plasma is a perfect pump for incoming neutrals, i.e. neutral pressure at the plasma is zero.

Now let I_n = Neutral beam equivalent current of H^+, amps.

S = Pumping speed of beam line pump, ltr.sec^{-1}

$2L$ = Length of input tube, cms.

C = Gas conductance of half the input tube, ltr.sec.$^{-1}$

n_1, n_3, n_4, n_5 = Flows in Torr ltr.sec.$^{-1}$ at room temperature.

γ = Molecules evolved from the wall per incident ion.

n_2 = Gas flow introduced by the deflected ions, Torr ltr.sec.$^{-1}$ at room temperature.

f = Fraction of beam that is re-ionised.

If all pressures are in Torr, at room temperature then

$$n_1 + n_3 = n_5 \quad .. (1)$$

$$n_3 + n_4 = n_2 \quad .. (2)$$

$$n_4 = P_2 C \quad .. (3)$$

$$n_5 = P_1 S \quad .. (4)$$

Gas desorbed by bombardment $= \frac{\gamma I_n f}{e}$ mol.sec.$^{-1}$ .. (5)

Let β = mol. per Torr ltr. at room temperature.

Then $n_2 = \frac{\gamma I_n f}{e \beta}$ .. (6)

As the source gas efficiency is assumed constant, n_1 may be expressed as

$$n_1 = \frac{A I_n}{e} \text{ atoms.sec.}^{-1}$$

where A is a constant.

$$n_1 = \frac{A I_n}{2e} \text{ mol. sec.}^{-1}$$

$$n_1 = \frac{A I_n}{2e\beta} \text{ Torr ltr.sec.}^{-1} \quad .. (7)$$

$$n_3 = (P_2 - P_1)C \quad .. (8)$$

Substitute (7), (8) and (4) in (1)

$$P_2 C = P_1(S + C) - \frac{A I_n}{2e\beta} \quad .. (9)$$

Substitute (8), (3) and (6) in (2)

$$2P_2 C = \frac{\gamma I_n f}{e\beta} + P_1 C \quad ..(10)$$

The re-ionisation target, T, is given by,

$$T = \left\{ \frac{(P_2 + P_1)}{2} L + \frac{P_2 L}{2} \right\} \times \alpha \text{ mol.cm}^{-2}$$

where α = mol. cm^{-3} Torr^{-1} $= \frac{\beta}{10^3}$

$$\therefore T = \left\{ P_2 + \frac{P_1}{2} \right\} \frac{\beta L}{10^3} \quad ..(11)$$

Now $f = 1 - \exp[-\sigma T]$

$$\therefore \ell n \left\{ \frac{1}{1-f} \right\} = \sigma T \quad ..(12)$$

Substitute for P_2 from (9) into (10),

$$2P_1(S+C) - \frac{A I_n}{e\beta} = \frac{\gamma I n f}{e\beta} + P_1 C$$

$$P_1 = \frac{I_n}{e\beta} \left\{ \frac{\gamma f + A}{2S + C} \right\} \quad ..(13)$$

Substitute for P_2 from (10) into (11),

$$T = \left\{ \frac{\gamma I_n f}{e\beta 2C} + P_1 \right\} \frac{\beta L}{10^3} \quad ..(14)$$

Substitute (14) in (12) and (13) into the result,

$$\ell n \left\{ \frac{1}{1-f} \right\} = \frac{\sigma \beta L}{10^3} \left\{ \frac{\gamma I n f}{e\beta 2C} + \frac{I_n \gamma f}{e\beta(2S+C)} + \frac{I_n A}{e\beta(2S+C)} \right\}$$

$$I_n = \frac{10^3 e}{\sigma L} \ell n \left\{ \frac{1}{1-f} \right\} \left\{ \frac{2C(2S+C)}{(2S+3C)\gamma f + 2AC} \right\}$$

$$I_n = \frac{2 \cdot 10^3 Ce}{\sigma L \gamma f} \ell n \left\{ \frac{1}{1-f} \right\} / \left\{ 1 + \frac{2C}{(2S+C)} + \frac{2AC}{\gamma f(2S+C)} \right\}$$

The beam reaching the torus, $I_T = I_n (1-f)$, is given by

$$I_T = I_M \frac{(1-f)}{f} \ell n \left\{ \frac{1}{1-f} \right\} / \left\{ 1 + \frac{2C}{(2S+C)} + \frac{2AC}{\gamma f(2S+C)} \right\}$$

where $I_M = \frac{2 \cdot 10^3 Ce}{\sigma L \gamma}$ is the maximum possible transmitted equivalent beam current.

The Riviere and Sheffield analysis leads to the following formula,

$$I_T = \frac{10^3 C^1 e}{2\gamma L \sigma} \frac{(1-f)}{f} \ell n \left\{ \frac{1}{1-f} \right\} / \left\{ 1 + \frac{AC^1}{2\gamma f(C+2S)} \right\}$$

where C^1 is the effective pumping speed for the removal of gas from the centre of the pipe, ltr.sec.$^{-1}$ For the case $S \gg C$, then $C^1 \sim 2C$. Then,

$$I_T = \frac{I_M}{2} \frac{(1-f)}{f} \ln \left\{ \frac{1}{1-f} \right\} / \left\{ 1 + \frac{A\,C}{\gamma f(C+2S)} \right\} .$$

The most obvious difference between the two treatments is that the maximum possible transmitted equivalent beam current is a factor two higher in the present analysis. This is mitigated to some extent by the factor two in the last term of the denominator.

3. EXAMPLES

(a) For DITE tokamak, if the pumping system is outside the toroidal coil system, the shortest, widest input tube is ~120 cm long and 25 cm in diameter. An attainable pumping speed for a beam line on DITE is 1.5×10^5 ltr.sec.$^{-1}$ using a liquid helium cryo-pump. The energy considered optimum for H atoms injected into DITE is 30 keV where the ionisation cross section is 1.6×10^{-16} cm^2 per molecule of H_2[2]. The value of A depends on the source efficiency, the divergence of the beam and the geometry of the beam line. If only one pumping station is used in the beam line, A could be as high as 10. Using the above parameters, the power reaching the torus is plotted in Figure 2 as a function of the fractional loss for various values of γ. Shown for comparison is the result from the Riviere and Sheffield formula with $\gamma = 1$ and the result for simple re-ionisation, $\gamma = 0$.

(b) For a toroidal reactor, blanket and coil thickness will lead to input tube lengths >200 cm, and access between the coils will restrict the tube to a rectangular cross section ~ 100 cm x ~ 50 cm. For these dimensions the tube conductance is ~ 5×10^4 ltr.sec.$^{-1}$ for D_2. If we have a 1 MeV deuterium beam, $\sigma \sim 2 \times 10^{-17}$ cm^2 mol.$^{-1}$ [2]. Now if we assume A ~ 4, γ = 1 mol.per ion, S = 2.5×10^5 ltr.sec.$^{-1}$ and the fractional loss is less than 5%, then $I_T \leq 550$ Amps. For a 500 keV deuterium beam $\sigma \sim 6 \times 10^{-17}$ cm^2 mol.$^{-1}$ [2] and fractional losses of less than 5%, then $I_T \leq 190$ Amps.

4. CONCLUSIONS

The problem of the transmission of intense neutral beams through a tube immersed in a magnetic field has been re-examined and inconsistencies in the earlier treatment removed by the present analysis. Although a more favourable result than the earlier treatment is obtained, the problem remains significant. It is obvious that if high transmission efficiencies are to be obtained adequate pumping must be provided and input tube wall materials with low γ values chosen.

5. REFERENCES

1. Transfer Efficiency of Intense Neutral Beams. A C Riviere and J Sheffield. Nuclear Fusion Vol. 15 (1975) 944-947.
2. Experimental Results on Charge-Charging of Hydrogen and Helium Atoms at Kinetic Energies above 0.2 keV. S K Allison, Reviews of Modern Physics, Vol. 30 No. 4 (1958) 1137-1168.

Fig. 1

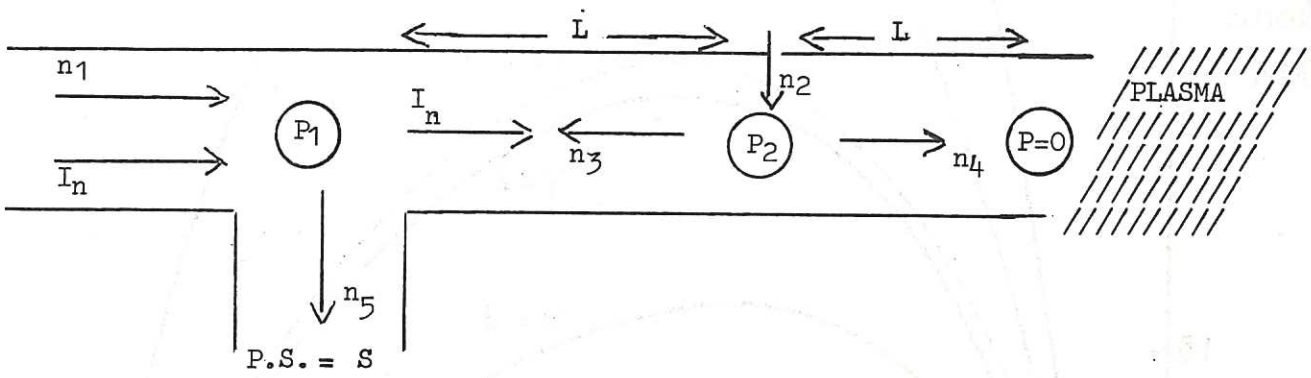

Fig. 2

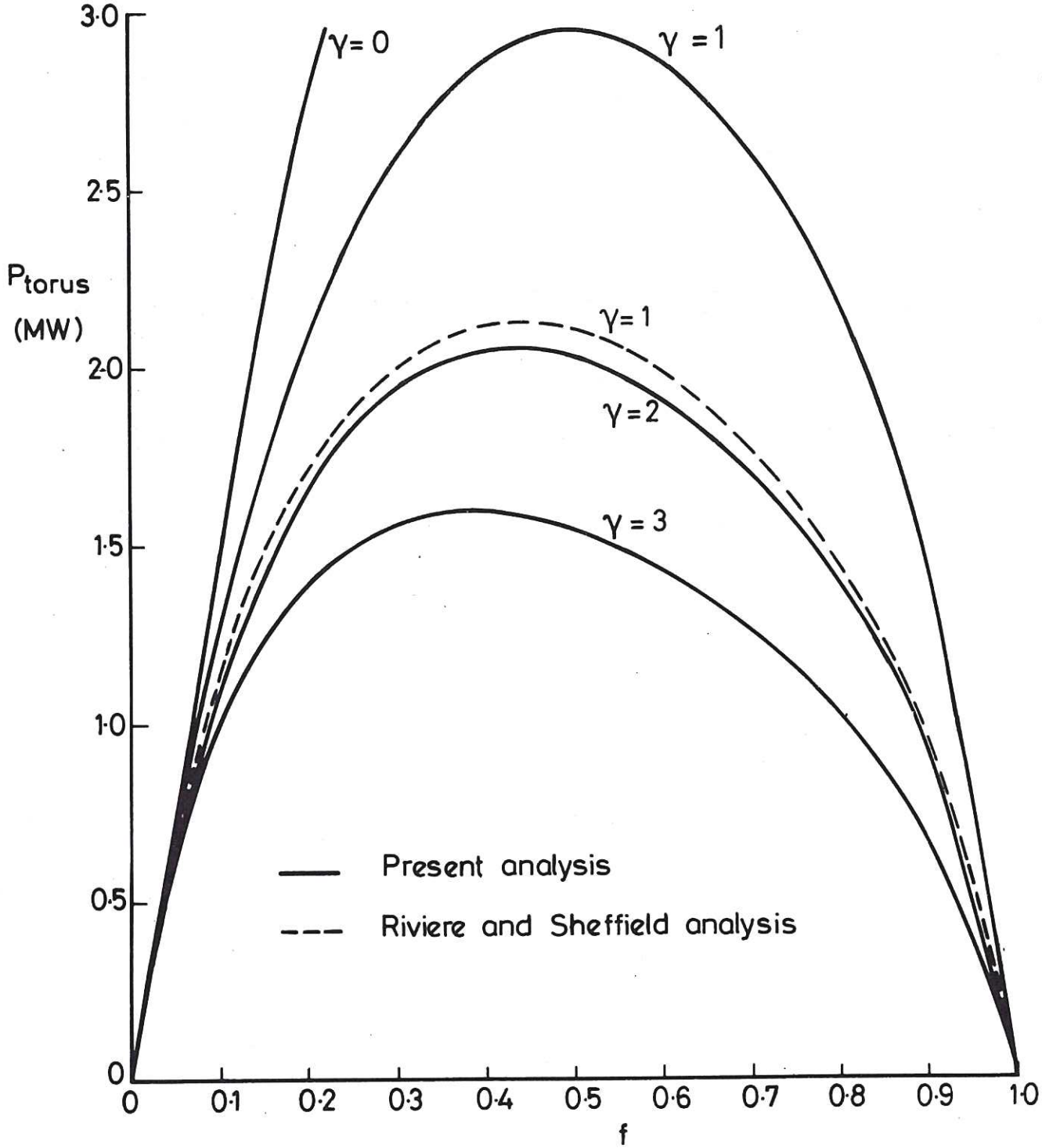

Power to torus v. fractional loss

HER MAJESTY'S STATIONERY OFFICE

Government Bookshops

49 High Holborn, London WC1V 6HB
13a Castle Street, Edinburgh EH2 3AR
41 The Hayes, Cardiff CF1 1JW
Brazennose Street, Manchester M60 8AS
Wine Street, Bristol BS1 2BQ
258 Broad Street, Birmingham B1 2HE
80 Chichester Street, Belfast BT1 4JY

Government publications are also available through booksellers

CLM - R 164

CLM - R 164

UKAEA

Report

TOROIDAL EQUILIBRIUM OF REVERSED FIELD PINCH

A MOHRI

CULHAM LABORATORY
Abingdon Oxfordshire

1977

Available from H. M. Stationery Office

C/18

£1.00

CLM-R 164

TOROIDAL EQUILIBRIUM OF REVERSED FIELD PINCH

A. MOHRI*

Culham Laboratory, Abingdon, Oxon, U.K.

(Euratom/UKAEA Fusion Association)

* On leave from Institute of Plasma Physics, Nagoya University, Japan.

SBN 85311 050 6

May 1977

SYNOPSIS

An analytical expression for the toroidal equilibrium of a reversed field pinch is derived in which the radial distribution of the plasma pressure is variable from a convex to a concave one near the magnetic axis. Using this expression, the marginal condition satisfying the Suydam's criterion for stability is found in the limiting case of large aspect ratio. The fraction of trapped particles in this configuration decreases near the periphery as the value of β becomes larger.

1. INTRODUCTION

Up to date the reversed field pinch (RFP) has been proved to have large potential to confine high β plasma.[1)2)] The essential feature of this configuration is its high magnetic shear. There is no restriction on the choice of large aspect ratio owing to the stabilising effect of the high magnetic shear. However, in general the toroidal magnetic configuration is apt to be deformed by the finite β of the confined plasma. In order to discuss the change of the configuration of the RFP due to the toroidicity and the finite β, a suitable and simple analytical expression would be preferred, in which the pressure gradient of the plasma should be adjustable since it is an essential variable for discussions of the stability of plasma.[3)] Experiments in ZETA and HBTX-I[1)2)] have shown that the stable configuration of the RFP is situated close to the state of the force free Bessel function model of the linear cylindrical geometry.[4)5)] Also this stable state satisfies Suydam's necessary condition[6)] for the plasma stability.[1)2)] The marginal condition of this criterion has been found numerically by using a relaxation method.[7)]

In this report, an analytical expression of the toroidal equilibrium of the RFP is presented, where the profile of the pressure can be changed widely. The Suydam criterion and the fraction of trapped particles in this model are also given.

2. EXPRESSION OF EQUILIBRIUM STATE

The equation of the magnetohydrostatic equilibrium for axisymmetric toroidal plasma is written in the quasi-toroidal coordinates (ρ,θ,ϕ) depicted in Fig.1 as

$$\frac{\partial^2\psi}{\partial\rho^2} + \frac{1}{\rho}\frac{\partial\psi}{\partial\rho} + \frac{1}{\rho^2}\frac{\partial^2\psi}{\partial\theta^2} + \frac{1}{2}\frac{d}{d\psi}f^2 + \mu_o R\frac{dp}{d\psi}$$

$$= \frac{1}{R}\left[\frac{\partial\psi}{\partial\rho}\cos\theta - \frac{1}{\rho}\frac{\partial\psi}{\partial\theta}\sin\theta\right] - 2\mu_o R\rho\frac{dp}{d\psi}\cos\theta \qquad (1)$$

to the order of the inverse aspect ratio ρ/R, where R is the major radius of the torus and ψ the magnetic flux function. The scalar plasma pressure p and the current stream function f are arbitrary function of ψ. Using the normalisations

$$\psi = B_o R a\Phi\ ,\ p = p_o P(\Phi),\ f^2 = B_o{}^2R^2F^2(\Phi),\ \rho = ar,\ \varepsilon = a/R,$$

we have a dimensionless form of Eq.(1)

$$\frac{\partial^2\Phi}{\partial r^2} + \frac{1}{r}\frac{\partial\Phi}{\partial r} + \frac{1}{r^2}\frac{\partial^2\Phi}{\partial\theta^2} + \frac{1}{2}\frac{d}{d\Phi}(F^2 + \alpha P)$$

$$= \varepsilon\left[\frac{\partial\Phi}{\partial r}\cos\theta - \frac{1}{r}\frac{\partial\Phi}{\partial\theta}\sin\theta - \alpha r\frac{dP}{d\Phi}\cos\theta\right], \qquad (2)$$

where

$$\alpha = p_o / (B_o{}^2/2\mu_o)$$

is a parameter concerning the beta of the plasma. In this case, the magnetic field $\vec{B} = B_o\vec{b}$ and the current $\vec{J} = (B_o/a\mu_o)\vec{j}$ are

$$\vec{b} = (b_r,\ b_\theta,\ b_\phi) = \frac{1}{1+\varepsilon r\cos\theta}\left(\frac{1}{r}\frac{\partial\Phi}{\partial\theta},\ -\frac{\partial\Phi}{\partial r},\ F\right), \qquad (3)$$

and

$$\vec{j} = (j_r,\ j_\theta,\ j_\phi)$$

$$= \left(\frac{1}{2F}\frac{dF^2}{d\Phi} b_r,\ \frac{1}{2F}\frac{dF^2}{d\Phi} b_\theta,\ \frac{1}{2}\left\{(1+\varepsilon r\cos\theta)\alpha\frac{dP}{d\Phi} + \frac{1}{1+\varepsilon r\cos\theta}\frac{dF^2}{d\Phi}\right\}\right). \quad (4)$$

The radial profile of the plasma pressure is an essential variable for discussing the stability, so that an expression for the profile is desired which can be varied. Equation(3) means that the function $F(\Phi)$ should be reversed to express the RFP configuration. For these reasons, we choose the following forms of F and P

$$F(\Phi) = \mu(\Phi + A),$$

$$P(\Phi) = \mu^2\left(\{\Phi + D\} - \eta\{\Phi + D\}^2 \right),$$

where μ is a parameter of the configuration, and A and D are constants decided by the boundary condition. The pressure profile can be changed by the parameter η. The case $\eta = 0$ has been discussed in ref[8]. We consider the boundary condition that the pressure P vanishes at $r = 1$. Then, the solution of Eq.(2) where magnetic surfaces are circular can be found to the order of ε as

$$\Phi = J_o(\mu k r) + \varepsilon S\cos\theta, \quad (5)$$

where

$$S = \frac{1}{2}\left[rJ_o(\mu k r) - \frac{J_o(\mu k)}{J_1(\mu k)} J_1(\mu k r)\right]$$

$$+ \frac{\alpha}{k^2}\left[\{1+2\eta J_o(\mu k)\}\left\{\frac{J_1(\mu k r)}{J_1(\mu k)} - r\right\} + \frac{1}{2}\eta\mu k(r^2-1)J_1(\mu k r)\right], \quad (6)$$

$$k^2 = 1 - \alpha\eta. \quad (7)$$

Also we have

$$F = \mu[J_0(\mu kr) - \frac{1}{2}\alpha\{1 + 2\eta J_0(\mu k)\} + \varepsilon S\cos\theta], \tag{8}$$

$$P = \mu^2[J_0(\mu kr) - J_0(\mu k) + \varepsilon S\cos\theta][1 - \eta\{(J_0(\mu kr) - J_0(\mu k) + \varepsilon S\cos\theta\}]. \tag{9}$$

The boundary condition of the plasma pressure is satisfied since the function S vanishes at r = 1. The magnetic field outside the plasma can easily be found by connecting analytically the internal field with the outer vacuum field on the intersurface r = 1. The toroidal effect $\varepsilon S\cos\theta$ in Eq.(5) includes in itself the influence of finite plasma pressure (or finite α) as is seen in Eq.(6). The function F is also changed by α and η so that the condition of the field reversal is modified by them.

Parameters which are frequently used in the linear configuration $\varepsilon = 0$ are easily derived from Eqs.(3) and (5) to (9). 'Pinch ratio' defined by $\theta \equiv B_\theta\ (\rho = a)/\langle B_\phi \rangle$, where $\langle X \rangle$ means the average of X over the cross section of the plasma, is

$$\theta = \frac{b_\theta(r=1)}{\langle b_\phi \rangle} = \frac{\mu}{2} k^2 [1 - \frac{\mu k C}{2J_1(\mu k)}]^{-1}, \tag{10}$$

where

$$C = \frac{\alpha}{2} [1 + 2\eta J_0(\mu k)].$$

'Field parameter' defined by $B_\phi(\rho = a)/\langle B_\phi \rangle$ is

$$\lambda = \frac{b_\phi(r=1)}{\langle b_\phi \rangle} = \frac{\mu k[J_0(\mu k) - C]}{2J_1(\mu k) - \mu k C}\ . \tag{11}$$

The value of β at the centre r = 0 for $\varepsilon = 0$, β_0, and the average

of β, $\bar{\beta}$, are related with α such that

$$\beta_o = \alpha \cdot \frac{[1-J_o(\mu k)]\cdot[1-\eta\{1-J_o(\mu k)\}]}{[1 - C]^2} \tag{12}$$

and

$$\bar{\beta} = \frac{\langle p\rangle}{\langle \frac{B^2}{2\mu_o}\rangle} = \alpha \frac{\langle p\rangle}{\langle b^2\rangle} = \alpha \cdot \frac{[\frac{2J_1(\mu k)}{\mu k} - J_o(\mu k)][1+2\eta J_o(\mu k)] - \eta J_1^2(\mu k)}{(k^2+1)[J_1^2(\mu k)+J_o^2(\mu k)]+C^2 - \frac{2}{\mu k}[2C+ k^2 J_o(\mu k)]J_1(\mu k)}. \tag{13}$$

The average poloidal β is also found to be

$$\bar{\beta}_p \equiv \frac{\langle p\rangle}{\frac{B_\theta^2(r=1)}{2\mu_o}} = \frac{\langle P\rangle}{b_\theta^2(r=1)}$$

$$= \frac{\alpha}{k^2 J_1^2(\mu k)} [\{2 \frac{J_1(\mu k)}{\mu k} - J_o(\mu k)\}\cdot\{1+2\eta J_o(\mu k)\}-\eta J_1^2(\mu k)]. \tag{14}$$

The pitch of a field line s is

$$s \equiv \frac{\rho B_\phi}{B_\theta} = \frac{r b_\phi}{b_\theta} = \frac{\mu k r [J_o(\mu k r) - C]}{k^2 J_1(\mu k r)} \tag{15}$$

In the case of the linear force-free state ($\varepsilon = 0$, $\alpha = 0$), θ and λ are reduced to the Bessel function model of J.B.Taylor; i.e. $\theta = \frac{1}{2}\mu$ and $\lambda = \frac{1}{2}\mu J_0(\mu)/J_1(\mu)$. θ, λ and β_o for $\eta = 0$ are all in agreement with the results in ref.[8].

3. DEPENDENCE OF THE CONFIGURATION ON PARAMETERS

Let us define a critical value of η:

$$\eta_c = \frac{1}{2} \frac{1}{1 - J_o(\mu k)}, \tag{16}$$

then the radial profile of the pressure for $\varepsilon \to 0$ becomes

convex for $\eta < \eta_c$

and

concave for $\eta > \eta_c$ near the centre axis.

At $\eta = \eta_c$ the profile becomes flat at the centre $r = 0$ where $d^2P/dr^2 = 0$, and the pressure vanishes at the centre if $\eta = 2\eta_c$. In the range $\eta_c < \eta < 2\eta_c$ the position of the peak of the pressure r_0 is related to η as

$$\eta = \frac{1}{2} \frac{1}{J_0(\mu k r_0) - J_0(\mu k)}$$

The toroidal field at the boundary $r = 1$ is

$$B_\phi(r=1) = [J_0(\mu k) - C]/(1 + \varepsilon\cos\theta)$$

so that the field reversal of the toroidal magnetic field occurs if

$$J_0(\mu k) \leq \frac{\alpha}{2(1 - \alpha\eta)} . \qquad (17)$$

The necessary value of μ for the field reversal becomes smaller as α and/or η increases.

Profiles of B_ϕ, B_θ, p and s for different α and η in the case $\varepsilon = 0$ are presented in Fig.2 where the maxima of B_ϕ, p and s are normalised to unity and B_θ is shown relative to the maximum of B_ϕ. The value of μk is fixed at $\mu k = 2.2$. The toroidal magnetic field is not reversed in the force-free state $\alpha = 0$ in which the field parameter $\lambda = +0.218$ and $\theta = 1.1$ (see Fig.2(a)). The field parameter decreases as α(i.e. β) becomes higher and then the field reversal occurs at higher α satisfying the inequality (17). Figure 2(b) and (c) show this RFP state where $\eta = \eta_c = 0.562$. Examples of the case $\eta_c < \eta < 2\eta$ are also shown in Fig.2(d) and (e).

The (usual) magnetic axis relative to the geometrical axis r = 0 is shifted by

$$\Delta r = \frac{\varepsilon}{(\mu k)^2}\left[1 - \frac{\mu k J_0(\mu k)}{2J_1(\mu k)} + \frac{2\alpha}{k^2}\left\{ \frac{\mu k}{2J_1(\mu k)} - 1 + 2\eta \left(\frac{\mu k}{2J_1(\mu k)} - 1\right) J_0(\mu k) - \frac{\mu^2 k^2}{8} \right\}\right], \quad (18)$$

toward the outside of the torus from r = 0. Figure 3 shows the dependence of this shift on μ, β_0 and η. In the force-free case the shift monotonically increases as the parameter μk becomes larger, while it turns to have a minimum with appropriate higher values of β_0 and/or η.

The second magnetic axis closed by extraordinary magnetic surfaces appears on the inside of the torus ($\theta = \pi$) if the following condition is attained;

$$\alpha \geq k^2 \frac{\left(\frac{1}{\varepsilon} - \frac{1}{2}\right) J_1^2(\mu k) + \frac{1}{2} J_0(\mu k) J_2(\mu k)}{J_2(\mu k) + \eta\{2J_0(\mu k) J_2(\mu k) - J_1(\mu k)\}} \quad . \quad (19)$$

The appearance of the second magnetic axis would limit the available region of the RFP operation within the frame of this model as the problem of large β_p in tokamak.[9)10)] However, the condition (19) is only satisfied on high μ side where the field parameter λ becomes very large.[8)] For this reason, the problem is not serious in the usual operation of the RFP.

From Eqs. (3),(4),(8) and (9) we have

$$\left.\begin{aligned} j_r &= \mu b_r, \\ j_\theta &= \mu b_\theta, \\ j_\phi &= \frac{1}{2}(1 + \varepsilon r\cos\theta)\alpha\frac{dP}{d\Phi} + b_\phi \cdot \frac{dF}{d\Phi} \quad . \end{aligned}\right\} \quad (20)$$

Therefore, it is sufficient to show b_ϕ, b_θ, P and j_ϕ in order to see the toroidal effect. These components on the median plane of the torus ($\theta = 0, \pi$) are shown in Fig. 4 for several sets of

the parameters. The aspect ratio $1/\varepsilon$ is set to 3 which is the planning value of HBTX-II[9], and the parameter μ is 2.6. In the force-free state $\alpha = 0$ (Fig. 4(a)), the toroidal field b_ϕ and the toroidal current j_ϕ become zero at the same radius, but these zero-crossing points separate as α increases (Fig. 4(b) and 4(c)). A striking toroidal effect can be seen in the profile of b_θ; b_θ on the inside of the torus is larger than that on the outside. However, as α or β becomes higher, b_θ decreases on the inside of the torus and it rises at the periphery on the outside. This change of b_θ with α affects the fraction of trapped particles, especially near the periphery.

4. TRAPPED PARTICLES

The absolute value of the magnetic field is found from Eqs. (3),(5) ~ (8) as

$$b^2 = (F^2 + R'^2) + 2\varepsilon[R'S' - r(F^2 + R'^2)]\cos\theta,$$

where $R = J_0(\mu kr)$ and X' means dX/dr. By using the average radius of any magnetic surface $\bar{r}$, the absolute value of the magnetic field on any $\bar{r}$ magnetic surface is found after some algebra to be

$$|b| = H^{1/2}(\bar{r})\left[1 + \varepsilon \frac{K(\bar{r})}{H(\bar{r})}\cos\theta\right], \qquad (21)$$

where

$$H(\bar{r}) = \mu^2[J_0^2(\bar{x}) + k^2 J_1^2(\bar{x}) - C\cdot\{2J_0(x) - C\}], \qquad (22)$$

$$K(\bar{r}) = -(\mu k)[J_0(\bar{x})J_1(\bar{x}) + \frac{1}{2}\bar{x}\{J_1^2(\bar{x}) + \frac{1+\alpha\eta}{k^2} J_0^2(\bar{x})\}]$$
$$+ \frac{\alpha(\mu k)}{k^2}[2J_1(\bar{x}) - \frac{\alpha}{4}\bar{x} - \eta\{x(J_1^2(\bar{x}) + \alpha J_0(\bar{x}) + \alpha\eta J_0^2(\mu k) - xJ_1^2(\bar{x})\}], \qquad (23)$$

$$\bar{x} = \mu k\bar{r}.$$

Then, the fraction of trapped particles on $\bar{r}$ magnetic surface is given by

$$\Omega(\bar{r}) = \sqrt{2\varepsilon}\left|\frac{K(\bar{r})}{H(\bar{r})}\right|^{\frac{1}{2}} \qquad (24)$$

The second term on the right hand side of Eq. (23) is an increasing function of α (up to $\alpha = 4J_1(\mu k)/(\mu k)$ for $\eta=0$), while the first term is negative. Therefore, finite α works to decrease the fraction of trapped particles. For $K \geq 0$ trapped particles on the inside of the torus come out.[2)10)11)8)] Figure 5 shows this effect of α for the case $\mu = 2.6$ and $\eta = \eta_c = 0.456$. The fraction decreases as β_0 becomes higher. The dotted curve $\Omega/\sqrt{2\varepsilon} = \bar{r}^{-1/2}$ roughly corresponds to the case of tokamak. In the inner region the fraction is close to this $\bar{r}^{-1/2}$ curve. The remarkable change of Ω near the periphery in the RFP mainly orignates in the large dependences of b_ϕ and b_θ on finite β.

5. CONFIGURATION SATISFYING SUYDAM'S CRITERION AT THE LIMIT OF LARGE ASPECT RATIO

Most of stable states obtained in ZETA lie in the region of λ - Θ space which is surrounded by Taylor's force-free state[5)]

and the curve from a high β model.[7] This high β model was used to find numerically the configuration of the RFP which marginally satisfies the Suydam's criterion everywhere inside the plasma region. The marginal condition is analytically given for the model used here.

The Suydam's necessary condition for stability[6] is written in our normalisation by

$$\alpha \frac{dP}{dr} + \frac{r}{4} b_\phi^2 \left(\frac{1}{s} \frac{ds}{dr} \right)^2 \geq 0 \qquad (25)$$

where s is the pitch given by Eq. (15). Using Eqs. (3),(5),(8), (9) and (15),we rewrite Eq. (25) as

$$[\{J_0(x) - C\}\{2 - \frac{xJ_0(x)}{J_1(x)} - xJ_1(x)\}]^2$$

$$\geq 4\alpha x J_1(x)[1 - 2\eta\{J_0(x) - J_0(\mu k)\}], \qquad (26)$$

where $x = \mu k r$ and $C = \frac{1}{2}\alpha\{1 + 2\eta J_0(\mu k)\}$.

The approximate form of the condition (26) for small x is

$$\frac{1}{64} (C^2 + 10C + 1 - 24\alpha\eta)x^2 \geq C - \alpha\eta. \qquad (27)$$

Above inequality is always satisfied if

$$\left.\begin{aligned} & C - \alpha\eta \leq 0 \quad \text{or} \quad \eta \geq \eta_c = \frac{1}{2} \frac{1}{1 - J_0(\mu k)}, \\ \text{and} \quad & \\ & (C^2 + 10C + 1 - 24\alpha\eta) \geq 0. \end{aligned}\right\} \qquad (28)$$

Thus, the marginal condition for small x is $\eta = \eta_c$ where the pressure profile is flat at the centre x = 0 as shown in Section 3. The requirement (28) also leads to the limit on α

$$\alpha \leq \alpha_s \equiv 0.0718/\eta_c \qquad (29)$$

whence

$$k^2 = k_s^2 \equiv 1 - \alpha_s \eta_c = 0.9282.$$

Therefore, once the parameter μ is given, the associated parameters in this marginal case can be found from

$$\begin{aligned}
\eta &= \eta_c = \frac{1}{2} \frac{1}{1 - J_0(\mu k_s)} , \\
\theta &= \theta_s \equiv \frac{0.481(\mu k_s)}{1 - 0.0359 \dfrac{(\mu k_s)}{J_1(\mu k_s)}} \\
\lambda &= \lambda_s \equiv \frac{(\mu k_s)[J_0(\mu k_s) - 0.0718]}{2J_1(\mu k_s)[1 - 0.0359 \dfrac{(\mu k_s)}{J_1(\mu k_s)}]} \\
\beta_o &= \beta_{os} \equiv 4.04 \alpha_c^2 .
\end{aligned} \tag{30}$$

It is numerically shown that the condition (26) is satisfied all over the region $0 \leq r \leq 1$ if above marginal condition $\eta = \eta_c$ and $\alpha = \alpha_s$ for small x is used. In Fig. 6(a), the marginal curve on $\lambda - \theta$ space is shown and the numerical result from the high β model[7] is also drawn for comparison. The region between this analytical curve and the curve of the force-free Bessel function model is narrow compared with the case of the high β model. This shrinkage of the region is due to the modest pressure gradient near the periphery in our case. Figure 6(b) shows the relation of β_{os} with θ_s. At $\mu = 3.2$, β_{os} becomes 0.13.

The requirement that there is 'no pitch minimum' inside the plasma region leads to the condition

$$c \geq \frac{2J_0(x)J_1(x) - x\{J_0^2(x) + J_1^2(x)\}}{2J_1(x) - xJ_0(x)}$$

Since the right hand side is always negative and $C \geq 0$, the requirement is always satisfied in our case. The variation of the pitch s is shown in Fig. 2.

Another stability criterion concerning the magnetic shear on the axis[12] is

$$\gamma = \frac{1}{2} s \frac{d^2 s}{dr^2} \Big|_{r \to 0} < -\frac{4}{9} = -0.444 \qquad (31)$$

In our model

$$\gamma = -\frac{1 - C^2}{2k^3} \qquad (32)$$

and in the marginal case for the Suydam's criterion we have

$$\gamma = -\frac{1 + \alpha_s \eta_c}{2(1 - \alpha_s \eta_c)^2} = -0.622.$$

Therefore, the criterion (31) is satisfied.

6. SUMMARY

An analytical expression for the toroidal equilibrium of the RFP has been presented. The profile of the plasma pressure in this model is variable from a peaked profile to a hollow one, and the configuration tends to the force-free Bessel function model as β tends to zero. With this expression, toroidal effects have been demonstrated in the profiles of the magnetic field and the pressure. The fraction of trapped particles is also found. The marginal condition for the Suydam's criterion has been given in this model and compared with the numerical result using the relaxation method.

ACKNOWLEDGEMENT

The author would like to thank Dr. H.A.B.Bodin, Dr. A.A.Newton and Dr. D.C.Robinson for kind suggestions and helpful discussions. He is much indebted to Dr. R.S.Pease for providing him with the chance to enjoy working at the Culham Laboratory.

REFERENCES

1) Reviewed in: H.A.B. Bodin, Confinement in High-beta plasma; Lecture 2-p.71 The Reversed Field Pinch. To be published in Proceedings of Erice Summer School on Pulsed Fusion Reactors, Erice, Trapani, Sicily (September 1974). H.A.B. Bodin, 3rd Topical Conference on Pulsed High Beta Plasmas (Culham, 1975) B1.1.

2) E.P. Butt, C.W. Gowers, R.F. Gribble, Yin-An Li, A.A. Newton, D.C. Robinson, J.C. Taylor, W.J. Sharp, A.J. Verhage, H.A.B. Bodin, 5th Int. Conference on Plasma Physics and Controlled Nuclear Fusion, (Tokyo, 1974) CN-33/E9.2.

3) D.C. Robinson, Plasma Phys. 13 (1971) 439.

4) D. Voslamber and D.K. Callebaut, Phys. Rev., 128 (1962) 2016.

5) J.B. Taylor, 5th Int. Conference on Plasma Physics and Controlled Nuclear Fusion (Tokyo, 1974) CN-33/PD-1.

6) B.R. Suydam, Int. Conference on Peaceful Uses of Atomic Energy, 31 (1958) 157.

7) A.A. Newton, Li Yin-An, J.W. Long and B.C. Yeung, 3rd Topical Conference on Pulsed High Beta Plasmas (Culham, 1975) B2.6.

8) A. Mohri, ibid. B2.3.

9) H.A.B. Bodin, private communication.

10) D.C. Robinson, private communication.

11) J.W. Connor, F.A. Haas and C. Ll. Thomas, private communication.

12) D.C. Robinson, Symposium on Closed Confinement Systems (Dubna, September 1969) paper 52c.

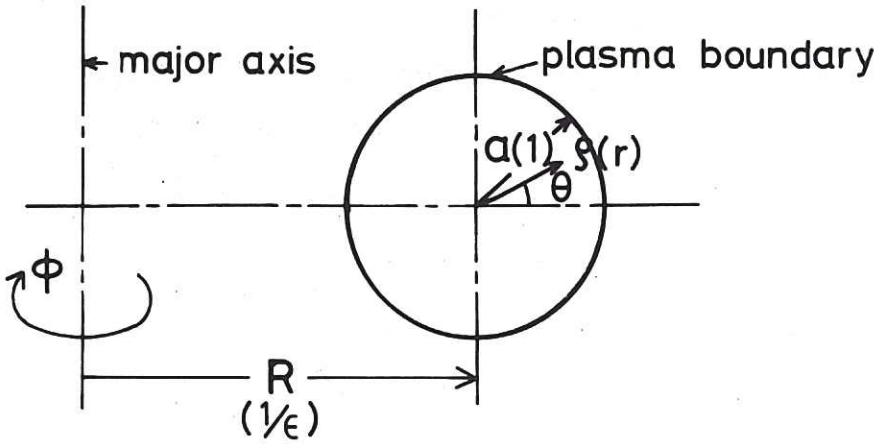

Fig.1 Quasi-toroidal coordinates (ρ,θ,ϕ). In the parentheses their normalised coordinates are given.

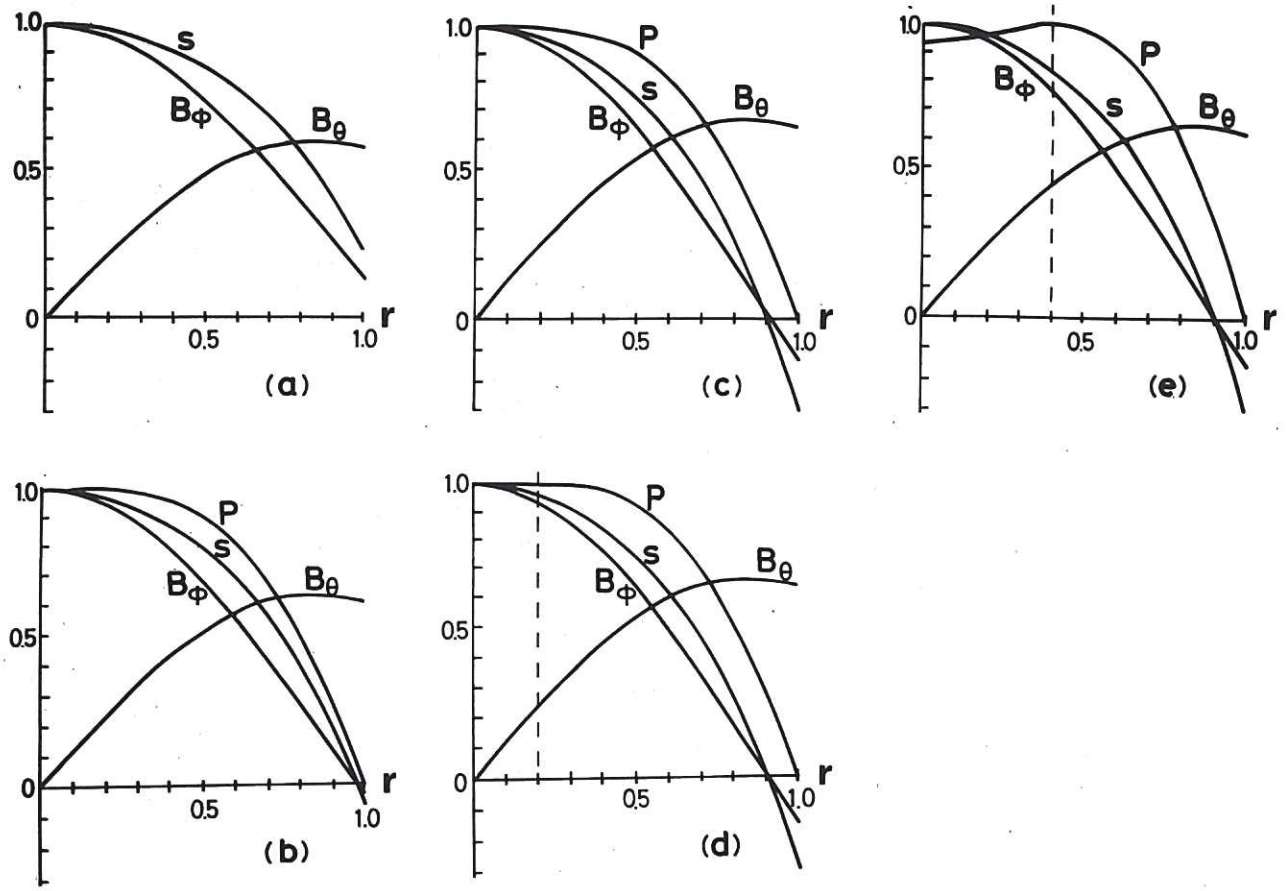

Fig.2 Radial distributions of the toroidal field B_ϕ, the poloidal field B_θ and the pitch s at the limit of the large aspect ratio ($\epsilon = 0$). B_ϕ and s are normalised to be 1.0 at the centre and B_θ is relative value to B_ϕ at the centre. The parameter μ is set to be 2.2 for all cases. (a) $a = 0, \eta = 0, \theta = 1.1, \lambda = 0.218, \beta_o = 0$. (b) $a = 0.25, \eta = \eta_c = 0.562, \theta = 1.41, \lambda = -0.083, \beta_o = 0.15$. (c) $a = 0.4, \eta = \eta_c = 0.562, \theta = 1.74, \lambda = -0.40, \beta_o = 0.30$. (d) $a = 0.4, \eta = 1.06\eta_c = 0.594, \theta = 1.74, \lambda = -0.415, \beta_o = 0.28$. (e) $a = 0.4, \eta = 1.26\eta_c = 0.709, \theta = 1.72, \lambda = -0.441, \beta_o = 0.22$.

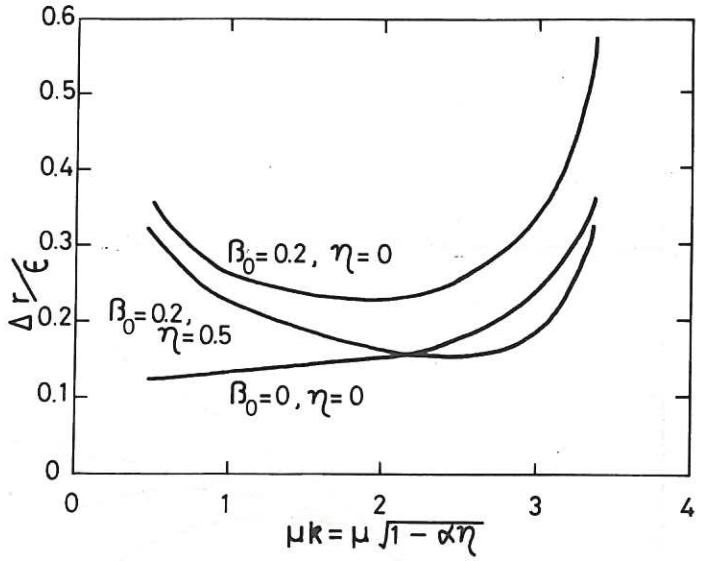

Fig.3 Shift of the magnetic axis Δr as a function of μk for different values of β_o and η.

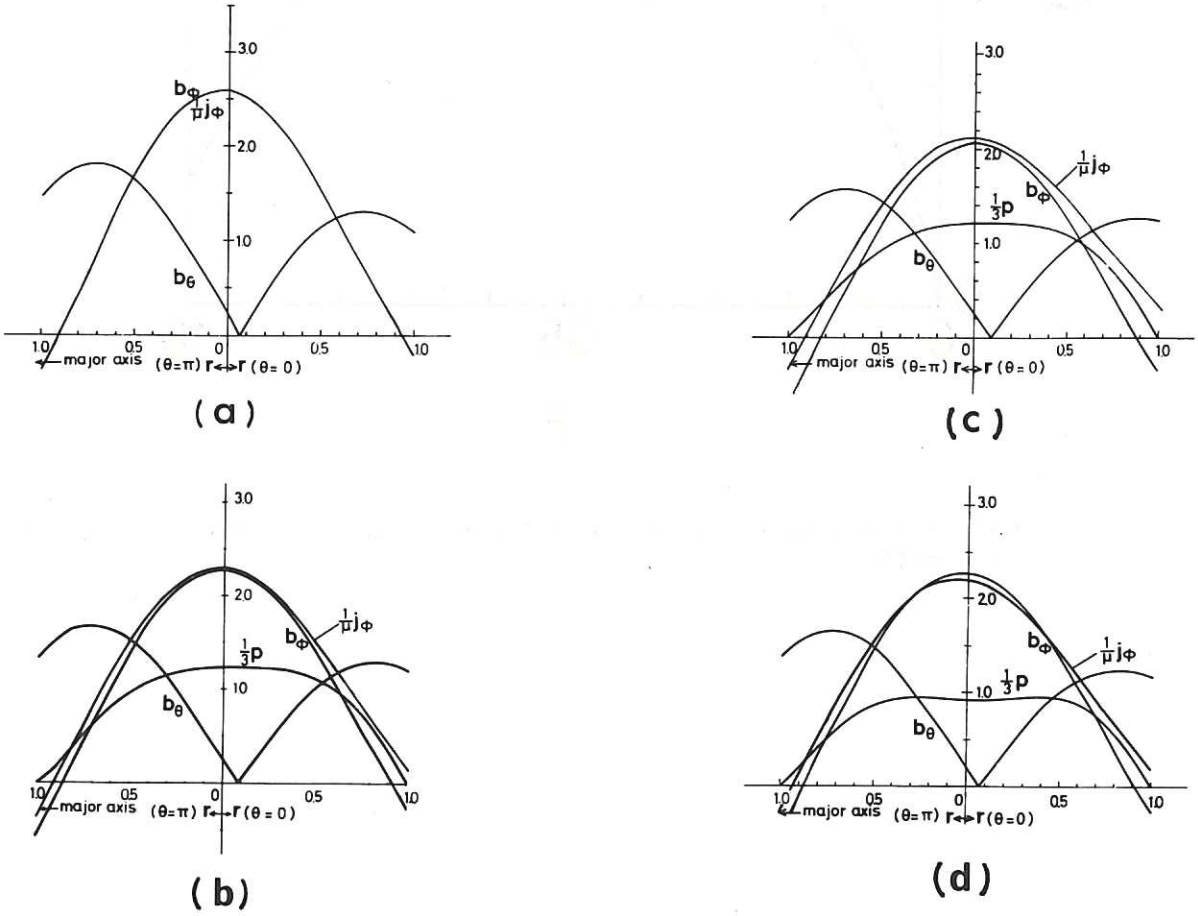

Fig.4 Profiles of the toroidal field b_ϕ, the poloidal field b_θ the pressure P and the toroidal current j_ϕ on the median plane of the torus for $\epsilon = 1/3$ and $\mu = 2.6$. (a) $\alpha = 0, \eta = 0, \theta = 1.3, \lambda = -0.267, \beta_o = 0, \beta_p = 0$. (b) $\alpha = 0.25, \eta = \eta_c = 0.456, \theta = 2.08, \lambda = -0.49, \beta_o = 0.177, \beta_p = 0.338$. (c) $\alpha = 0.4, \eta = \eta_c = 0.456, \theta = 2.92, \lambda = -0.71, \beta_o = 0.343, \beta_p = 0.532$. (d) $\alpha = 0.25, \eta = 1.3\eta_c = 0.592, \theta = 2.15, \lambda = -0.399, \beta_o = 0.134, \beta_p = 0.295$.

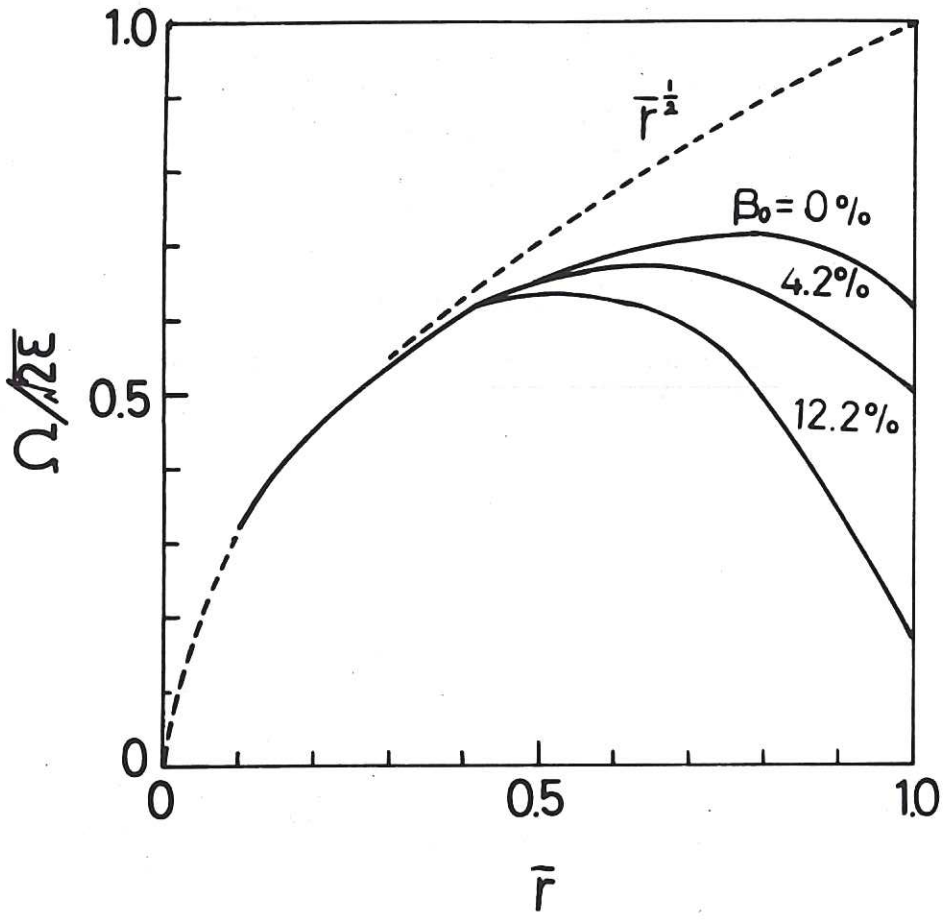

Fig.5 Fractions of trapped particles in the RFP configuration for $\mu = 26$ and $\eta = \eta_c = 0.456$.

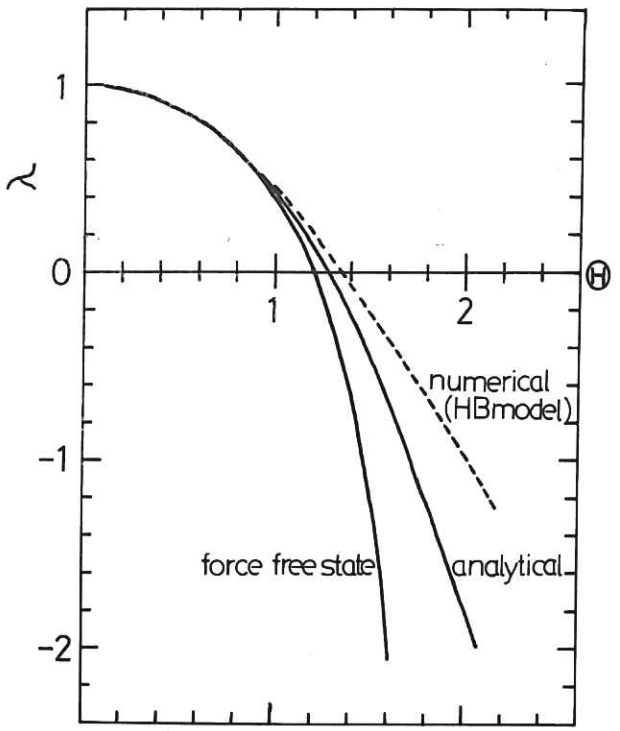

Fig.6 (a) Marginal curve of the Suydam's necessary condition for stability. The dotted line is the numerical result by the relaxation method (ref.7).

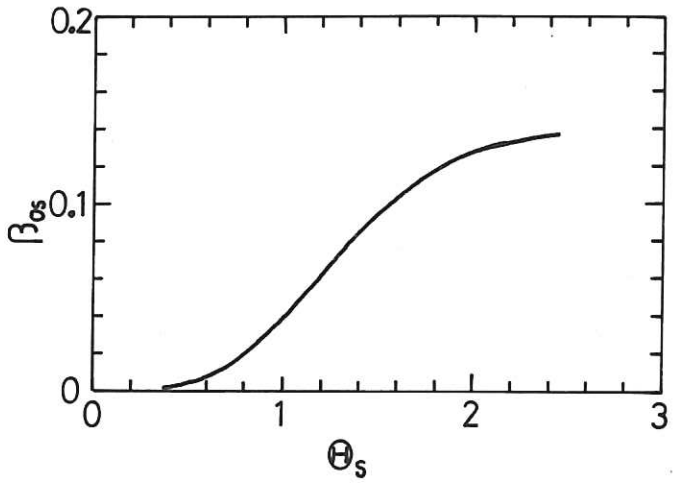

Fig.6 (b) Relation between β_{os} and θ_s in the marginal condition.

HER MAJESTY'S STATIONERY OFFICE

Government Bookshops

49 High Holborn, London WC1V 6HB
13a Castle Street, Edinburgh EH2 3AR
41 The Hayes, Cardiff CF1 1JW
Brazennose Street, Manchester M60 8AS
Wine Street, Bristol BS1 2BQ
258 Broad Street, Birmingham B1 2HE
80 Chichester Street, Belfast BT1 4JY

Government publications are also available through booksellers